This is a pre-print version of the journal paper:

Characterising the compressive anisotropic properties of analogue bone using optical strain measurement

A. Marter[1], A. Dickinson[1], F. Pierron[2], Y.K.K. Fong[1], M. Browne[1]*

[1] Bioengineering Science Research Group, Faculty of Engineering and Physical Sciences, University of Southampton, Southampton SO17 1BJ, UK
[2] Engineering Materials Research Group, Faculty of Engineering and Physical Sciences, University of Southampton, Southampton SO17 1BJ, UK

*** Corresponding Author: doctor@soton.ac.uk**
Mailpoint M7,
Bioengineering Science Research Group,
University of Southampton,
Highfield,
Southampton,
SO17 1BJ,
United Kingdom

Tel: +44(0)2380593279

Keywords:
Analogue Bone; Polyurethane Foam; Material Characterisation; Mechanical Testing; Compression Testing

Word Count:
2491 (Introduction – Discussion).

1. Abstract

The validity of conclusions drawn from preclinical tests on orthopaedic devices depends upon accurate characterisation of the support materials: frequently, polymer foam analogues. These materials often display anisotropic mechanical behavior, which may considerably influence computational modelling predictions and interpretation of experiments. Therefore, the present study sought to characterise the anisotropic mechanical properties of a range of commonly used analogue bone materials, using non-contact multi-point optical extensometry method to account for the effects of machine compliance and uneven loading. Testing was conducted on commercially available 'cellular', 'solid' and 'open cell' Sawbone blocks with a range of densities. Solid foams behaved largely isotropically. However, across the available density range of cellular foams, the average Young's modulus was 23-31% lower ($p<0.005$) perpendicular to the foaming direction than parallel to it, indicating elongation of cells with foaming. The average Young's modulus of open celled foams was 25-59% higher ($p<0.05$) perpendicular to the foaming direction than parallel to it. This is thought to result from solid planes of material that were observed perpendicular to the foaming direction, stiffening the bulk material. The presented data represent a reference to help researchers design, model and interpret tests using these materials.

2. Introduction

Polymer foams have been extensively used in the testing and development of orthopaedic devices and corresponding computational models [1-5]. Often these foams are used in preference to cadaver and animal material, with researchers noting their relative low cost, availability, the consistency of material properties, avoidance of ethical concerns, and their ease of handling and storage [6]. A range of polymer foam types is available commercially (Sawbones, Pacific Research Labs, Malmö, Sweden), as both anatomically shaped bone models and standard blocks, to represent a range of bone types. The mechanical properties of polymer foams may be adjusted by means of porosity content, to cover a range of natural bone stiffness. However, the polymer expands by 'foaming' during manufacture which may result in an uneven aspect ratio of the foam structural features (i.e. cells), and consequent anisotropic mechanical behaviour, and will lead to varying mechanical behaviour dependent on the orientation of testing [7, 8].

A number of studies have evaluated the mechanical properties of polyurethane (PU) foams in the context of a biological analogue, considering compressive [9-13], shear [13] and fatigue [14] properties. However, to the authors' knowledge their anisotropic material properties have not been reported, and may be of key importance to computational models and analogue material selection. Additionally, limited Poisson's ratio data is available for polyurethane (PU) foams commonly used as a biological analogue. In this study, the assumption of isotropy was tested both parallel and perpendicular to the foaming direction. Literature data indicates a wide range of Young's Modulus values for nominally the same material [11-13, 15, 16], which is highly dependent upon the experimental method employed. Therefore, testing was performed using a non-contact multi-point optical extensometry method that accounts for the effects of machine compliance and uneven loading. This method has previously been verified against the digital volume correlation method [15, 16].

3. Method

A range of sample types and densities was selected corresponding to a range of trabecular bone material properties spanning the majority of commercially available materials. Three different types of foam were tested (Figure 1): 'solid rigid polyurethane' (S), 'cellular rigid polyurethane' (C) and 'open cell rigid foam' (O, a composite made of urethanes, epoxies and structural fillers) (SAWBONES®, Malmö, Sweden). Where available, densities of each foam type were selected such that they were directly comparable between foam types (Table 1). All specimens were stored and tested in ambient environmental conditions.

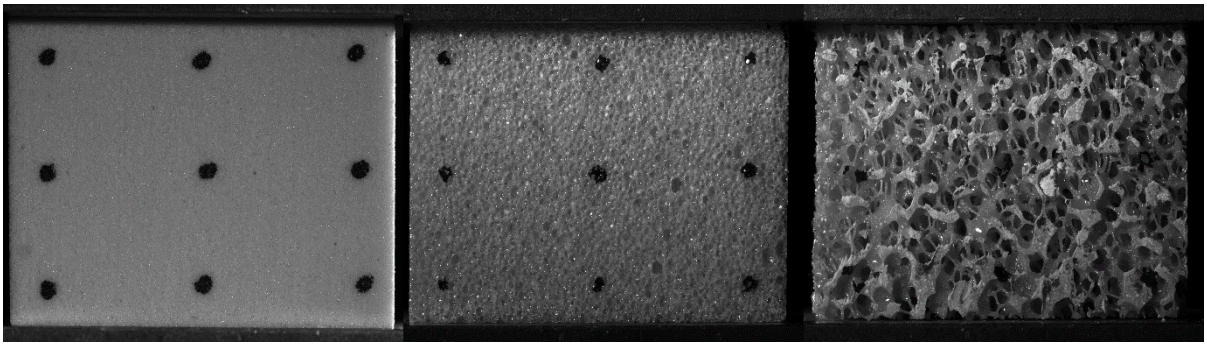

Figure 1 – Representative sample images for solid polyurethane (S, left), cellular polyurethane (C, centre) and open urethane-epoxy composite (O, right) foam types.

Foam Type	Manufacturer Product code	Quoted density (pcf)	Quoted density ($g.cm^{-3}$)	Yield Stress (MPa)	Maximum test load (N) (parallel to foaming direction)	Maximum test load (N) (perpendicular to foaming direction)
Cellular	1522-09	7.5	0.120	1.4	1821	1428
	1522-11	12.5	0.200	3.9	5072	3978
	1522-1300	15	0.240	4.1	5332	4182
	1522-12*	20	0.320	5.4	7023	5508
Solid	1522-536	8	0.128	1.5	1951	1530
	1522-48	12	0.192	3.2	4162	3264
	1522-02	15	0.240	4.9	6372	4998
	1522-03	20	0.320	8.4	10924	8568
	1522-04	30	0.480	18	23409	18360
Open	1522-524	15	0.240	0.67	871	683
	1522-526-1	20	0.320	1.3	1638	1284
	1522-525	30	0.480	3.20	4162	3264

Table 1 – Manufacturer-quoted test material properties, and test finish load. * The 20 pcf (0.306 $g.cm^{-3}$) cellular foam has glass fibre reinforcement. pcf: pounds per cubic foot.

Samples were cut to 40 x 51 x 51 mm (nominal dimensions) using a bandsaw, to adhere to testing standard ASTM D1621 – 10 in the foaming direction. The foaming direction was identified as the smallest 40mm 'thickness' dimension of the blocks as supplied by the manufacturer. Six specimens were tested for each foam type and density. The apparent density of each specimen was calculated by measurement of dimensions by digital calipers

and mass by electronic balance, with precisions of 0.01 mm and 0.0001 g respectively, in accordance with ASTM D1622 and compared with the manufacturer quoted densities.

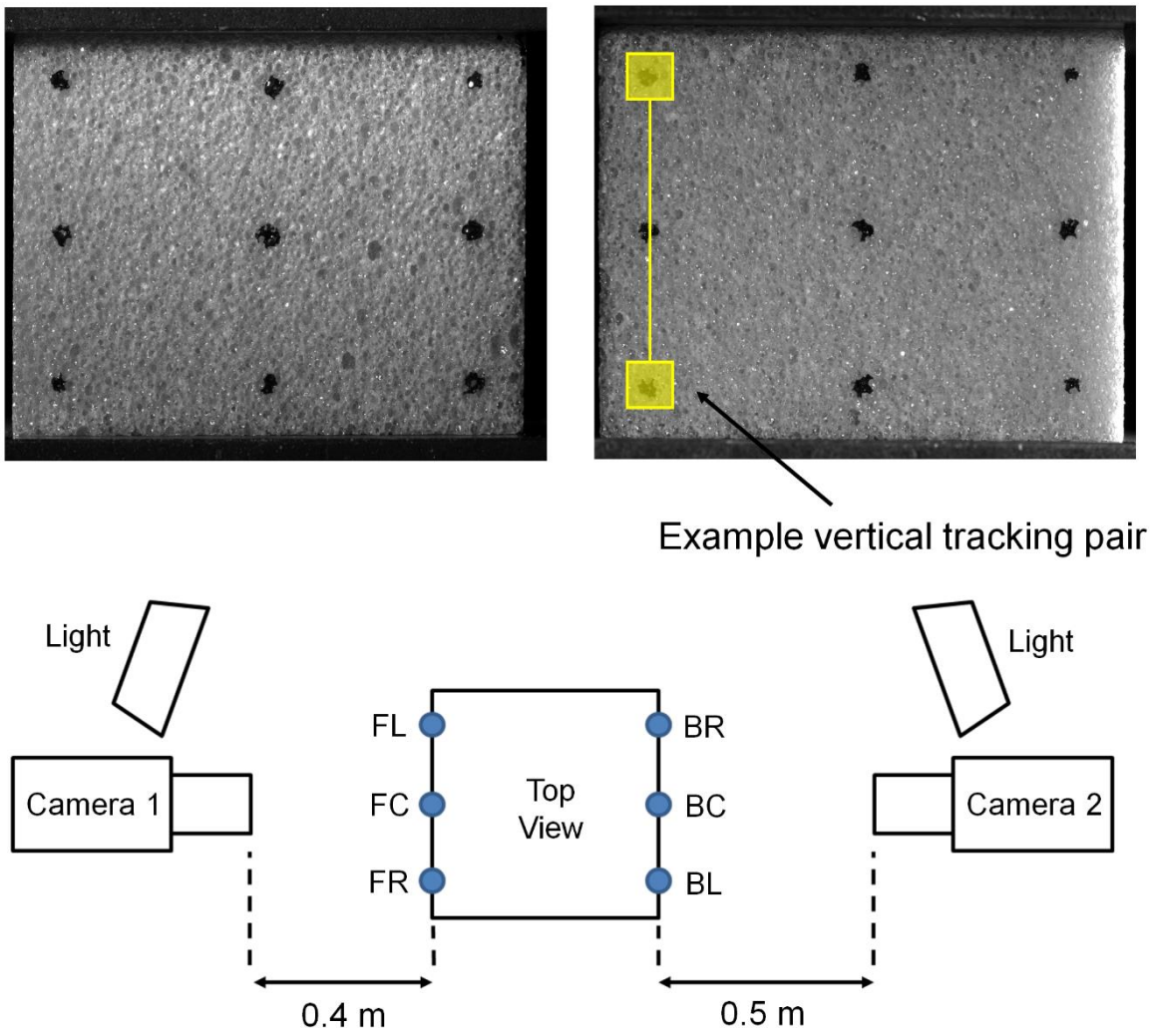

Figure 2 - Marker arrangement and experimental schematic for optical extensometry.

Each sample was compressed in a screw-driven electromechanical testing machine (Instron 5569, Instron, High Wycombe, UK). A displacement rate of 0.5 mm/min was selected to minimise test duration and limit image motion throughout testing. To maintain testing within the material's elastic behaviour range and thus enable testing of the same specimen in two directions, each specimen was loaded to half its documented yield stress (Table 1). Specimen deformation was measured by a non-contact optical extensometry method as described by Marter *et al.* (2017)[15, 16]. A grid of 9 markers was drawn onto the front and back surfaces of each specimen (Figure 2). These markers were then recorded throughout loading using two cameras (AVT Manta G504B, 2452 x 2056 pixels, 8-bit) fitted with a fixed focal length lens (Sigma 105mm f/2.8 EX DG Macro). Image exposure time was set to 1000 microseconds to minimise motion blur whilst maintaining image contrast. A laser cut acrylic template was used to ensure repeatability of point marker locations on the specimen's surface. The heterogeneous surface of the open cell samples complicated this marking procedure. Where markers could not be placed on the specimen surface, the material's surface structure was used to provide trackable features. The averaged strain response of the six vertical marker pairs was used to calculate specimen Young's Modulus. Poisson's ratio of each specimen was calculated as the ratio of the averaged central horizontal

marker pair's strain response divided by the averaged vertical strain response. The central horizontal markers pair were used to minimise the influence of friction at the specimen ends. Both Young's modulus and Poisson's ratio results were corrected to account for differences in surface to volumetric strains, not captured by point tracking, using an ANSYS finite element model [15, 16].

Anisotropy of each specimen was assessed by testing both along (parallel to) and perpendicular to the foaming direction, with the assumption that the material was transversely isotropic. As specimens were not cubic, maximum test loads for each loading direction were adjusted such that the final stress was equal for all tests (Table 1). Young's modulus and Poisson's ratio results were tested for normality using the Shapiro-Wilk test. For normally distributed data, a paired, 2 tailed t-test was used to test the null hypothesis that the materials had the same Young's modulus or Poisson's ratio parallel and perpendicular to the foaming direction, with a 95% significance level. For non-parametric data, a Wilcoxon signed-rank test was used.

4. Results

Cellular and solid foams had consistent densities (Table 2), with the standard deviation of density being small compared to the averaged measured value for each sample group (coefficient of variation <2%). The open cell foams were more heterogeneous (coefficient of variation 4-8%).

Foam Type	Quoted density ($g.cm^{-3}$)	Measured density Mean (SD) ($g.cm^{-3}$)
Cellular	0.120	0.115 (0.001)
	0.200	0.206 (0.001)
	0.240	0.248 (0.001)
	0.320	0.306 (0.001)
Solid	0.128	0.124 (0.001)
	0.192	0.183 (0.004)
	0.240	0.240 (0.000)
	0.320	0.311 (0.001)
	0.480	0.455 (0.004)
Open	0.240	0.239 (0.020)
	0.320	0.329 (0.012)
	0.480	0.461 (0.022)

Table 2 - Measured sample densities.

Foaming direction

Foams showed power law relationships ($R^2 > 0.97$) between the measured Young's modulus and density, for all foam types when tested in the foaming direction (Figure 3). The cellular foam followed a similar trend at lower densities, but the 0.306 $g.cm^{-3}$ density foam was an outlier, owing to its E-glass reinforcement, which was not present in the solid PU foam, or the other grades of cellular foam.

The cellular foams had 28-32% higher average Young's modulus than solid foams of equal density, with the exception of the fibre reinforced cellular 0.306 $g.cm^{-3}$ density foam which was 107% higher (Figure 3). The open cell foams had considerably lower modulus on

average than other foam types of same densities (23-55% that of solid foams). All differences were significant ($p < 0.005$, Table 3).

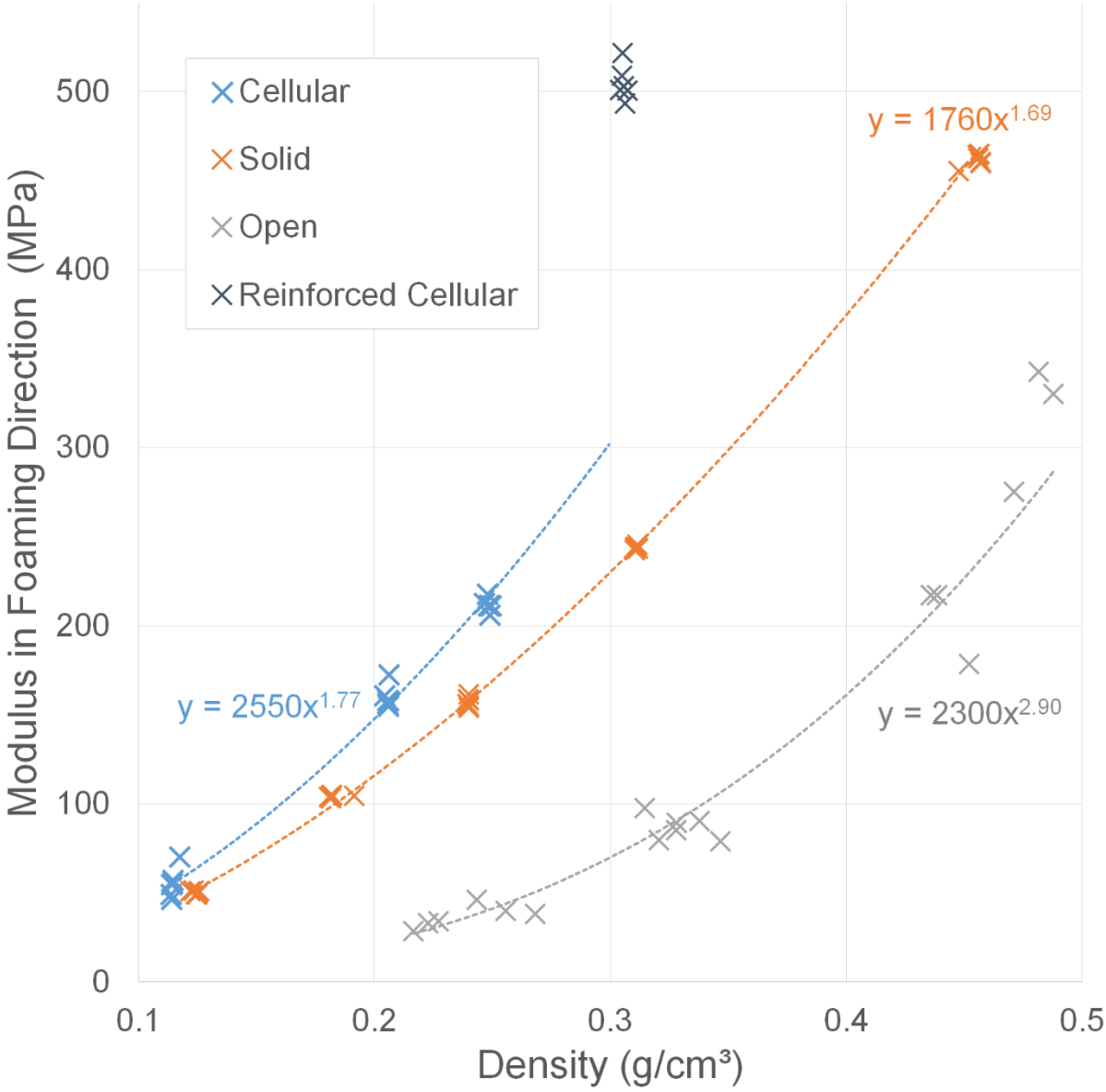

Figure 3 – Summary of all point tracking results for tested foam types and densities compressed in the foaming direction. Note: 0.306 g.cm^{-3} density cellular foam excluded from power law regression due to inclusion of fibre reinforcement

Perpendicular to foaming direction

A power law relationship was also observed (R^2>0.98) between the measured Young's modulus and density for all foam types when tested perpendicular to the foaming direction (Figure 4). Again, the 0.306 g.cm^{-3} density cellular foam was an outlier to this trend. Cellular foams had 0-16% lower average Young's modulus than solid foam types with the same densities, with the exception of the fibre reinforced cellular 0.306 g.cm^{-3} density foam, which was 43% higher. Open cell foams had lower moduli on average; however, the differences were less pronounced (39-72% of the solid foam modulus). All differences were significant ($p < 0.005$).

The measured Young's modulus of cellular foam specimens compressed perpendicular to the foaming direction was on average 23-31% lower than when compressed

parallel to the foaming direction ($p < 0.005$, Table 3) (Figure 5), with increased anisotropy at lower densities. Solid foam grades had no significant modulus differences between testing directions ($p > 0.1$). Open celled foams had the reverse relationship to cellular foams, with a Young's modulus on average 29-59% higher perpendicular to the foaming direction than parallel to it ($p < 0.05$).

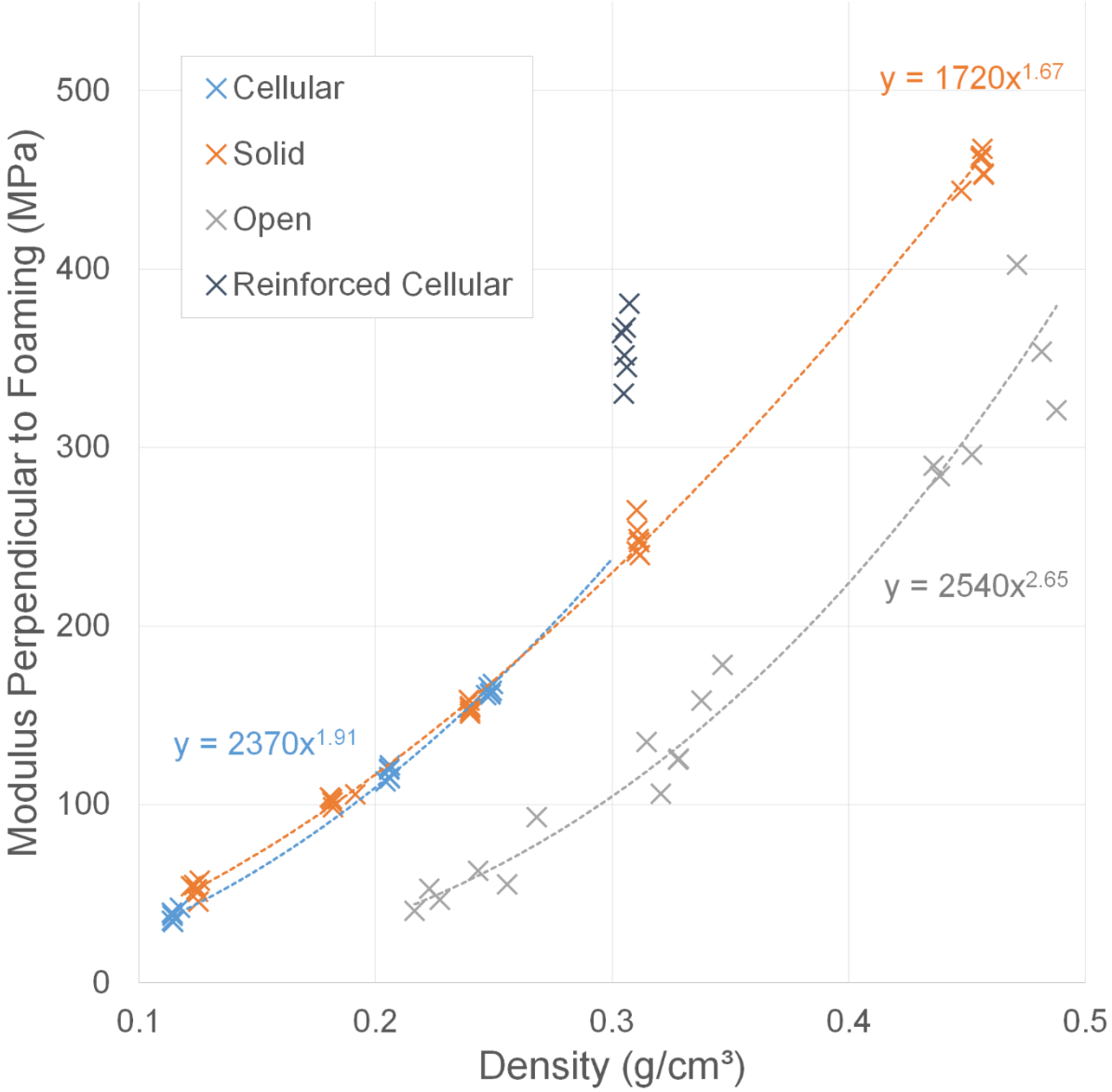

Figure 4 – Summary of all point tracking results for tested foam types and densities compressed perpendicular to the foaming direction. Note: 0.306 g.cm^{-3} density cellular foam excluded from power law regression due to inclusion of fibre reinforcement.

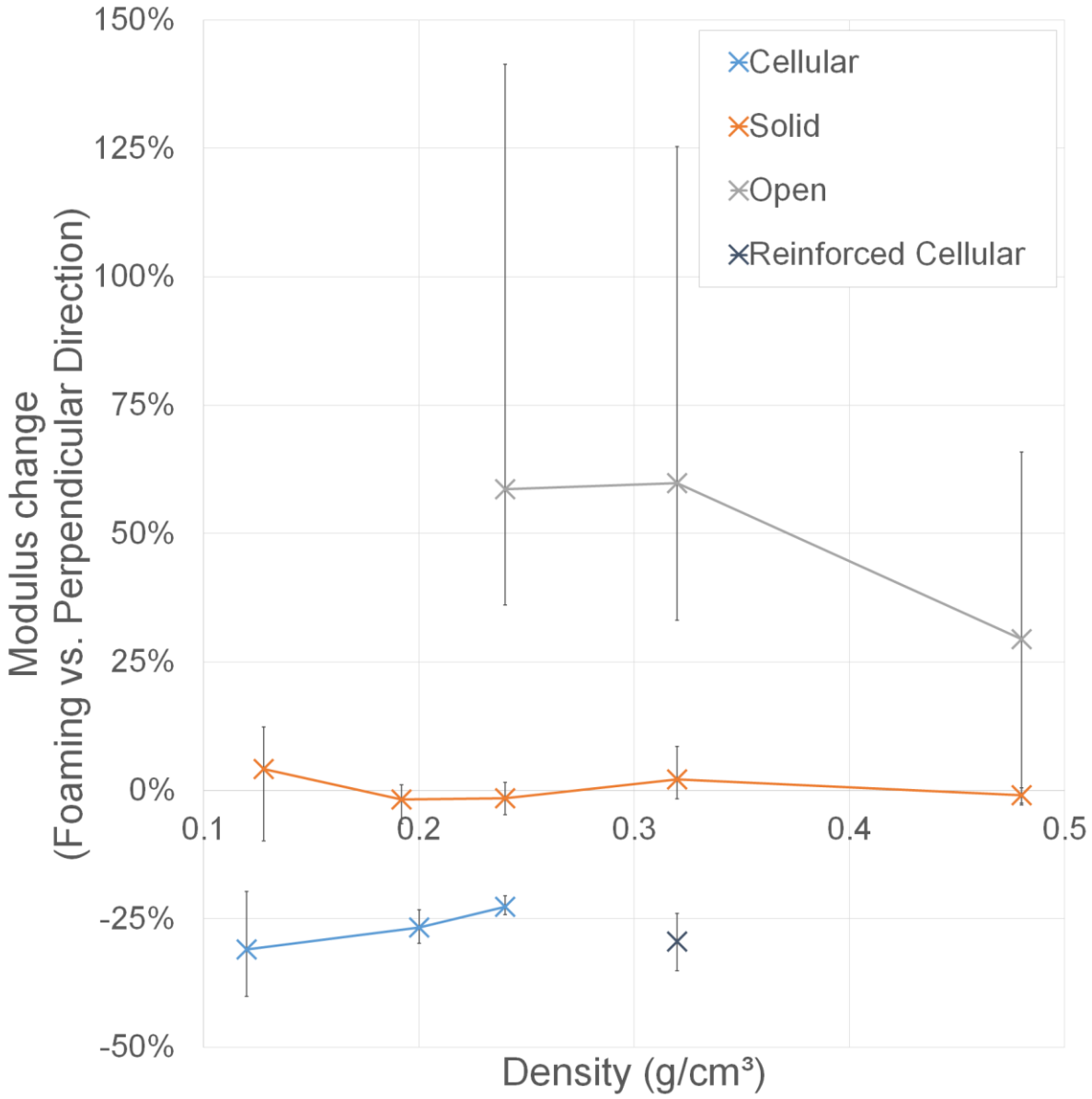

Figure 5 – Percentage modulus differences between foams tested in the foaming and perpendicular directions for each foam type and density grouping. Error bars show range (min-max).

Poisson's ratio

Poisson's ratios of cellular foams were consistently higher when tested in the foaming direction (Table 3), decreasing with increasing density. As solid foams were more isotropic, the Poisson's ratios were consistent between testing directions and densities. Open cell foams had a higher Poisson's ratio in the foaming direction, converging to that of the transverse direction at higher densities.

Foam Type	Nom. Density		Young's modulus results Mean (SD), MPa			Poisson's ratio results Mean (SD)		
	(pcf)	($kg.m^{-3}$)	Foaming	Transverse	significance	Foaming	Transverse	significance
Cellular	7.5	115	55.5 (8.27)	38.8 (2.95)	**0.002***	0.41 (0.077)	0.33 (0.020)	**0.033***
	12.5	206	160 (6.40)	120 (3.60)	**0.028*[1]**	0.39 (0.023)	0.31(0.008)	**0.000***
	15	248	212 (3.81)	164 (2.49)	**0.000***	0.34 (0.023)	0.31 (0.011)	**0.033***
	20†	306	505 (9.70)	357 (17.9)	**0.000***	0.33 (0.021)	0.28 (0.054)	**0.028*[1]**
Solid	8	124	50.5 (0.83)	52.6 (4.06)	0.231	0.31 (0.003)	0.34 (0.033)	0.345[1]
	12	183	104 (0.68)	103 (2.50)	0.180	0.34 (0.005)	0.31 (0.013)	**0.004***
	15	240	157 (2.83)	155 (3.08)	0.193	0.32 (0.005)	0.30 (0.007)	**0.001***
	20	311	244 (0.93)	249 (9.10)	0.206	0.31 (0.003)	0.32 (0.009)	0.083
	30	455	461 (3.55)	457 (8.66)	0.128	0.32 (0.002)	0.31 (0.010)	0.055
Open	15	239	36.8 (6.14)	58.5 (18.5)	**0.022***	0.47 (0.067)	0.23 (0.074)	**0.002***
	20	329	87.0 (7.07)	138 (26.0)	**0.006***	0.31 (0.052)	0.24 (0.057)	0.051
	30	461	260 (66.8)	324 (46.1)	**0.035***	0.24 (0.076)	0.24 (0.041)	0.932

Table 3 - Summary of Young's Modulus and Poisson's ratio values calculated from each testing directions. pcf: pounds per cubic foot. † contains short glass fibre reinforcement. * statistically significant ($p < 0.05$). [1] non-parametric Wilcoxon signed-rank test.

5. Discussion and Conclusions

Young's modulus was found to fit a power law relation with density for each foam type tested, in agreement with trends found in literature [8, 12]. The outlier to this trend was the 0.306 g.cm^{-3} density cellular foam, owing to its E-glass reinforcement. The inclusion of glass reinforcement has been reported to cause similar increases in compressive modulus for both polyurethane [17] and epoxy foams [18]. The power law exponent of both solid and cellular foams was between 1 and 2, indicating a mixture of bending- and stretch-dominated loading behaviour, typically observed in closed cell foams [8]. The exponent of the open cell foam was larger than two, indicating bending-dominated deformation consistent with open cell foams [8].

Of the foam types tested, both the cellular and open cell foams were observed to have significantly different Young's moduli between loading directions. The modulus of cellular foams was higher in the foaming direction, indicating elongation of cells in this direction. For the non-reinforced cellular foams this effect was slightly reduced at higher densities, where pore sizes tend to be smaller [12, 19]. This implies that larger pore sizes promoted increased elongation, which has previously been observed by Gong *et al* 2005 [20]. The Young's modulus of open cell foams was found to be higher when tested perpendicular to the foaming direction than parallel to it. This is thought to result from solid planes of material present in specimens perpendicular to the foaming direction (Figure 6), which may have acted to stiffen the bulk material.

Cancellous bone displays considerable Young's modulus anisotropy, varying with location as a result of preferred trabecular orientation dictated by Wolff's law. The analogue bone materials in the current study demonstrated anisotropy ratios consistent with reported values[21] for real bone obtained from calcaneus and proximal femur locations, but lower anisotropy than observed from spinal and distal femur extraction sites.

Young's modulus and Poisson's ratio variation of cellular and solid foam types were low within batches. However, tested open cell samples had considerable density, modulus and Poisson's ratio variation. Inter- and intra-sample consistency was higher for the analogues than for real bone[21], except for the most dense tested Open celled foam. The larger Poisson's ratio of cellular foams compressed in the foaming direction is thought to result from cell elongation effects as longer cells are more flexible laterally. The Poisson's ratio of solid foams was consistent between testing directions and densities as solid foams were more isotropic. Open celled foams tended to exhibit a strain gradient as a result of higher constraint at one end.

The only study to the authors' knowledge that measured the Poisson's ratio of biomechanical analogue foam materials' was by Kelly and McGarry [22]. They tested 8 mm side length Sawbone specimens with a 320 kg.m^{-3} nominal density, cellular foam cubes, measuring transverse strain by video extensometry. They found Poisson's ratio values between 0.14 and 0.28, generally lower than the current study. This may result from the small specimen dimensions tested in their study, in which test machine platen friction effects would have constrained transverse deformation across a larger proportion of the specimen.

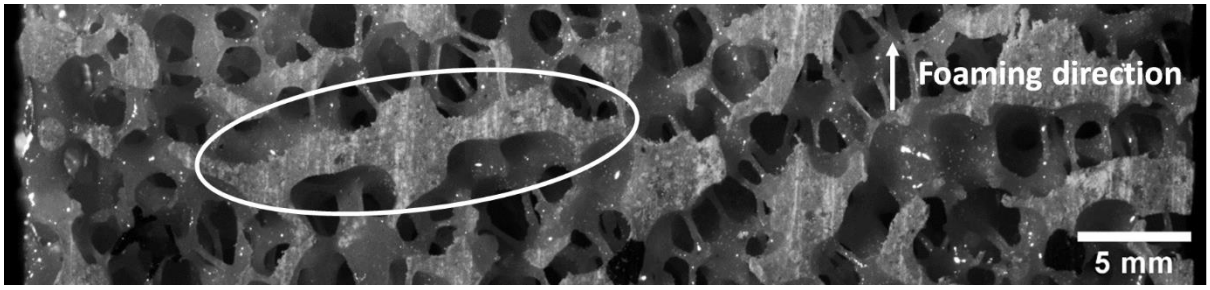

Figure 6 - Example of solid material plane present in some open cell foam specimens

Intra-sample variability of cellular and solid foams was low, and similar in both testing directions. The intra-sample variability was considerably higher for open cell foams. From Figure 3 and 4 it is apparent that most variation could be attributed to density differences. However, some variability is likely to result from the heterogeneous structure and solid planes of material.

This study made the assumption of transverse isotropy by testing Young's modulus in one plane perpendicular to the foaming direction only. Intra-sample specimens were machined from single blocks of material, so further variability might be observed between blocks and batches. Cubic specimens could not be produced with the ASTM D1621 – 10 specified 51 mm side length as only 40 mm thick blocks could be obtained. The non-contact optical strain estimation technique should minimize non-uniform loading and platen effects, but as a further mitigation measure, the larger 51 mm dimension was maintained for the non-foaming direction dimensions. Furthermore, bone may experience more complex loading including bending, tension and torsion, generating shear. The remit of this investigation was confined to compression, as the most common loading experienced by cancellous structures, and future work might characterise these materials' shear moduli.

In conclusion, the Young's modulus and Poisson's ratio of a range of commercially available analogue bone materials was characterised in compression both parallel and perpendicular to the foaming direction of production. Both the cellular and open celled foam types showed significant modulus changes between testing directions whilst solid foams did not. As such, the anisotropic properties of analogue bones should be carefully considered when selecting an appropriate analogue testing material. For example, if researchers are trying to represent a relatively isotropic anatomic site, the Solid foam material is appropriate. The Open and Cellular materials may be exploited to match the anisotropy of another anatomic site. Significant differences have been found between manufacturer-quoted and experimentally-obtained Young's Modulus values for nominally the same material, dependent on the testing technique employed [15, 16], and often the orientation of testing (perpendicular or parallel to the foaming direction) is not specified. Understanding these discrepancies becomes particularly relevant where the materials are used in Standards testing and pre-clinical analysis of medical devices. If these materials are used in implantation studies involving press-fit fixation without careful knowledge of the material's directional properties, corresponding uncertainty might be expected in the test results, such as the implantation force, implant and analogue deformations, and implant-analogue interface stability. Likewise, computational simulations employing these materials demand accurate input data, which can be acquired using a test technique which minimises experimental artefacts. The present work provides researchers with a database of values to this end.

6. Acknowledgements

This study's funding was provided by the following organisations:

- AM: The Engineering and Physical Sciences Research Council (EPSRC, grant EP/L505067/1) and DePuy Synthes.
- ASD: The Royal Academy of Engineering (RAEng, grant RF/130).

Supporting data are openly available from the University of Southampton repository at http://doi.org/10.5258/SOTON/D0281.
The Authors declare that there is no conflict of interest.

7. References

1. O'Laughlin R, Abbruzzese K, Lee D, Allan DG and Paliwal M. Failure analysis of surrogate tibial constructs with medium and fast setting bone cements. Engineering Failure Analysis. 2013; 32: 312-321.
2. Nagaraja S and Palepu V. Comparisons of anterior plate screw pullout strength between polyurethane foams and thoracolumbar cadaveric vertebrae. Journal of Biomechanical Engineering. 2016; 138: 104505.
3. Ferguson SJ, Weber U, von Rechenberg B and Mayer J. Enhancing the mechanical integrity of the implant-bone interface with bonewelding technology: Determination of quasi-static interfacial strength and fatigue resistance. J Biomed Mater Res B Appl Biomater. 2006; 77: 13-20.
4. Hsu J-T, Fuh L-J, Tu M-G, Li Y-F, Chen K-T and Huang H-L. The effects of cortical bone thickness and trabecular bone strength on noninvasive measures of the implant primary stability using synthetic bone models. Clinical Implant Dentistry and Related Research. 2013; 15: 251-261.
5. Wähnert D, Hofmann-Fliri L, Schwieger K, Brianza S, Raschke MJ and Windolf M. Cement augmentation of lag screws: An investigation on biomechanical advantages. Archives of Orthopaedic and Trauma Surgery. 2013; 133: 373-379.
6. Shim V, Boheme J, Josten C and Anderson I. Use of polyurethane foam in orthopaedic biomechanical experimentation and simulation. Polyurethane 1st ed: InTech. 2012: 171-200.
7. Gibson LJ and Ashby MF. Cellular solids: Structure and properties. Cambridge university press, 1999.
8. Hamilton AR, Thomsen OT, Madaleno LAO, Jensen LR, Rauhe JCM and Pyrz R. Evaluation of the anisotropic mechanical properties of reinforced polyurethane foams. Composites Science and Technology. 2013; 87: 210-217.
9. Szivek J, Thomas M and Benjamin J. Technical note. Characterization of a synthetic foam as a model for human cancellous bone. Journal of Applied Biomaterials. 1993; 4: 269-272.
10. Szivek JA, Thompson JD and Benjamin JB. Characterization of three formulations of a synthetic foam as models for a range of human cancellous bone types. Journal of Applied Biomaterials. 1995; 6: 125-128.
11. Patel PS, Shepherd DE and Hukins DW. Compressive properties of commercially available polyurethane foams as mechanical models for osteoporotic human cancellous bone. BMC Musculoskeletal Disorders. 2008; 9: 137.
12. Calvert KL, Trumble KP, Webster TJ and Kirkpatrick LA. Characterization of commercial rigid polyurethane foams used as bone analogs for implant testing. Journal of Materials Science: Materials in Medicine. 2010; 21: 1453-1461.
13. Thompson MS, McCarthy ID, Lidgren L and Ryd L. Compressive and shear properties of commercially available polyurethane foams. Journal of Biomechanical Engineering. 2003; 125: 732-734.
14. Palissery V, Taylor M and Browne M. Fatigue characterization of a polymer foam to use as a cancellous bone analog material in the assessment of orthopaedic devices. Journal of Materials Science: Materials in Medicine. 2004; 15: 61-67.
15. Marter A, Pierron F, Dickinson A and Browne M. Experimental methodologies for the accurate measurement of modulus values of analogue bone. Bone & Joint Journal Orthopaedic Proceedings Supplement. 2017; 99-B: 76-76.
16. Marter AD, AS; Pierron, F; Browne, M. A practical procedure for measuring the stiffness of foam like materials. Experimental Techniques. 2018; 42: 439-452.
17. Shen H and Nutt S. Mechanical characterization of short fiber reinforced phenolic foam. Composites Part A: Applied Science and Manufacturing. 2003; 34: 899-906.
18. Alonso MV, Auad ML and Nutt S. Short-fiber-reinforced epoxy foams. Composites Part A: Applied Science and Manufacturing. 2006; 37: 1952-1960.
19. Lee S-T and Ramesh NS. Polymeric foams: Mechanisms and materials. CRC press, 2004.
20. Gong L, Kyriakides S and Jang WY. Compressive response of open-cell foams. Part i: Morphology and elastic properties. International Journal of Solids and Structures. 2005; 42: 1355-1379.
21. Augat P, Link T, Lang TF, Lin JC, Majumdar S and Genant HK. Anisotropy of the elastic modulus of trabecular bone specimens from different anatomical locations. Medical Engineering and Physics. 1998; 20: 124-131.
22. Kelly N and McGarry JP. Experimental and numerical characterisation of the elasto-plastic properties of bovine trabecular bone and a trabecular bone analogue. Journal of the Mechanical Behavior of Biomedical Materials. 2012; 9: 184-197.